THE JOURNAL OF BIOLOGICAL CHEMISTRY VOL. 284, NO. 29, pp. 19580–19591, July 17, 2009

Corneal Dystrophy-associated R124H Mutation Disrupts TGFBI Interaction with Periostin and Causes Mislocalization to the Lysosome*[S]

Received for publication, March 27, 2009, and in revised form, April 27, 2009 Published, JBC Papers in Press, May 28, 2009, DOI 10.1074/jbc.M109.013607

Bong-Yoon Kim[‡§¶], James A. Olzmann[‖], Seung-il Choi[‡], So Yeon Ahn[‡], Tae-im Kim[‡¶], Hyun-Soo Cho[**], Hwal Suh[§¶], and Eung Kweon Kim[‡¶1]

*From the [‡]Corneal Dystrophy Research Institute and Department of Ophthalmology, the [§]Department of Medical Engineering, and the [¶]Brain Korean 21 Project Team of Nanobiomaterials for Cell-based Implants, College of Medicine, Yonsei University, 134 Shinchon-dong, Seodaemoon-gu, Seoul 120-752, South Korea, the **Department of Biology, College of Life Science and Biotechnology, Yonsei University, 134 Shinchon-dong, Seodaemoon-gu, Seoul 120-749, South Korea, and the [‖]Department of Biology, Stanford University, Stanford, California 94305-5020*

The 5q31-linked corneal dystrophies are heterogeneous autosomal-dominant eye disorders pathologically characterized by the progressive accumulation of aggregated proteinaceous deposits in the cornea, which manifests clinically as severe vision impairment. The 5q31-linked corneal dystrophies are commonly caused by mutations in the *TGFBI* (transforming growth factor-β-induced) gene. However, despite the identification of the culprit gene, the cellular roles of TGFBI and the molecular mechanisms underlying the pathogenesis of corneal dystrophy remain poorly understood. Here we report the identification of periostin, a molecule that is highly related to TGFBI, as a specific TGFBI-binding partner. The association of TGFBI and periostin is mediated by the amino-terminal cysteine-rich EMI domains of TGFBI and periostin. Our results indicate that the endogenous TGFBI and periostin colocalize within the *trans*-Golgi network and associate prior to secretion. The corneal dystrophy-associated R124H mutation in TGFBI severely impairs interaction with periostin *in vivo*. In addition, the R124H mutation causes aberrant redistribution of the mutant TGFBI into lysosomes. We also find that the periostin-TGFBI interaction is disrupted in corneal fibroblasts cultured from granular corneal dystrophy type II patients and that periostin accumulates in TGFBI-positive corneal deposits in granular corneal dystrophy type II (also known as Avellino corneal dystrophy). Together, our findings suggest that TGFBI and periostin may play cooperative cellular roles and that periostin may be involved in the pathogenesis of 5q31-linked corneal dystrophies.

Corneal dystrophies are characterized by the progressive loss of corneal transparency as a result of extracellular amyloid and non-amyloid deposits, which accumulate in different layers of corneal tissues. 5q31-linked corneal dystrophies are pathologically heterogeneous, autosomal-dominant disorders caused by mutations in the *TGFBI* (transforming growth factor-β-induced) gene, which encodes the TGFBI protein (also known as keratoepithelin or Big-H3) (1, 2). To date, more than 30 different mutations leading to corneal dystrophies have been attributed to mutations in *TGFBI*, the most frequent of which are mutations within exons 4 and 12, which result in amino acid substitutions in Arg^{124} and Arg^{555}, respectively (3, 4). The different mutations in TGFBI cause clinically distinct types of corneal dystrophies, which are classified according to the accumulation patterns of the deposits, including lattice corneal dystrophies type I and IIIA, deep stromal lattice corneal dystrophy, granular corneal dystrophies (GCDs)[2] type I and II (also known as Avellino corneal dystrophy), Reis-Bucklers corneal dystrophy (also known as corneal dystrophy of Bowman's layer type I), or Thiel-Behnke corneal dystrophy (also known as corneal dystrophy of Bowman's layer type II) (reviewed in Refs. 5 and 6). Histological examinations of corneal tissues demonstrate the presence of amyloid deposits in lattice corneal dystrophies and GCD II, hyaline accumulations in GCDs, and subepithelial fibrous material in Reis-Bucklers corneal dystrophy and Thiel-Behnke corneal dystrophy (7–14).

TGFBI was originally identified as a gene induced by transforming growth factor-β stimulation in adenocarcinoma cells and is expressed in many tissues (15). The human TGFBI consists of 683 amino acids, with the mature protein predicted to have a molecular mass of ~68 kDa. As shown in Fig. 1*A*, TGFBI contains an NH_2-terminal signal peptide that targets it for insertion into the lumen of the endoplasmic reticulum (ER) for eventual secretion, a cysteine-rich EMI domain, four tandem repeats of fasciclin-1 like (FAS1) domains, and a COOH-terminal RGD sequence (15–19). The FAS1 domains of TGFBI display homology to the cell adhesion protein fasciclin-I in *Drosophila*, an axon guidance protein that is involved in neuronal

* This study was supported by Korea Healthcare Technology R&D Project, Ministry for Health, Welfare, and Family Affairs, Republic of Korea, Grant A080320.

[S] The on-line version of this article (available at http://www.jbc.org) contains supplemental Figs. 1 and 2.

[1] To whom correspondence should be addressed: Dept. of Ophthalmology, College of Medicine, Yonsei University, 134 Shinchon-dong, Seodaemoon-gu, Seoul 120-752, South Korea. Tel.: 82-2-2228-3577; Fax: 82-2-312-0541; E-mail: eungkkim@yuhs.ac.

[2] The abbreviations used are: GCD, granular corneal dystrophy; FAS1, fasciclin 1; EMI, NH_2-terminal cysteine-rich domain of the EMILIN family; ECM, extracellular matrix; ER, endoplasmic reticulum; HCF, human corneal fibroblast; PBS, phosphate-buffered saline; NPCF, primary cultured corneal fibroblast from normal human; HCE, human corneal epithelial; TGN, *trans*-Golgi network; GFP, green fluorescent protein.

development (20). Based on the presence of multiple FAS1 domains, TGFBI has been assigned to a larger family of proteins, which includes periostin, stabilin-1, and stabilin-2 (16, 21). To date, many TGFBI homologues have been reported in various vertebrates, including mouse, chicken, pig, and zebrafish, but no homologues have been identified in invertebrates (16, 19, 21). TGFBI has been shown to interact with a number of extracellular matrix (ECM) proteins, including fibronectin, biglycan, decorin, and several types of collagen (19, 22–25). Furthermore, TGFBI also functions as a ligand for several integrins, including $\alpha 3\beta 1$, $\alpha v\beta 5$, $\alpha v\beta 3$, and $\alpha m\beta 2$ (26–29). The COOH-terminal RGD domain of TGFBI is the putative integrin-binding motif. However, several studies have suggested that the interactions between TGFBI and integrins are mediated via the YH (tyrosine-histidine) motifs and DI (aspartate-isoleucine) motifs present in the TGFBI FAS1 domains (30). Although the precise roles of TGFBI are not fully understood yet, emerging evidence suggests a role for TGFBI as a secreted factor involved in cell adhesion, proliferation, and migration.

TGFBI and periostin show a high degree of similarity in amino acid sequence and in overall domain structure, diverging primarily at the COOH terminus (Fig. 1*A*) (16, 21). Similar to TGFBI, periostin contains a NH_2-terminal secretory signal peptide followed by a cysteine-rich EMI domain, four tandem repeats of FAS1 domains, and a hydrophilic region in its COOH terminus (Fig. 1*A*) (16, 17, 31, 32). Periostin has been found to be ubiquitously expressed in multiple tissues in mammals (31, 33, 34). In addition, the expression of periostin has been implicated in the development of variety of cancers, including neuroblastoma, head and neck cancer, and non-small cell lung cancer, possibly by regulating the metastatic growth (32, 35). Periostin is also associated with epithelial-mesenchymal transition during cardiac development (36) and is induced during the proliferation of cardiomyocytes, thereby promoting cardiac repair after heart failure (37, 38). In addition, interlukin-4 and -13 have been found to induce the secretion of periostin from lung fibroblasts, implicating periostin in subepithelial fibrosis in bronchial asthma (39).

Despite the similarities between TGFBI and periostin, it is not known whether periostin is involved in the pathogenesis of 5q31-linked corneal dystrophies. In this study, we find that periostin specifically interacts with TGFBI via the NH_2-terminal cysteine-rich EMI domain and colocalizes with TGFBI in the *trans*-Golgi network of COS-7 and corneal fibroblast cells. In addition, corneal dystrophy-linked mutations in TGFBI disrupt its subcellular localization and impair its interaction with periostin. Furthermore, we find that periostin accumulates in extracellular corneal deposits in GCD II patients bearing homozygous R124H mutations in TGFBI. These findings provide new insights into the pathogenic mechanisms of TGFBI mutations in 5q31-linked corneal dystrophies and have important implications for understanding and treating corneal dystrophies.

EXPERIMENTAL PROCEDURES

Plasmids—pcDNA3-Periostin-GFP (34) and pcDNA3.1-Periostin-His (35) constructs were kind gifts from Dr. Hirokazu Inoue (Siga University of Medical Science, Japan) and Dr. Xiao-Fan Wang (Duke University, Durham, NC). Full-length human TGFBI cDNA was cloned into the pcDNA3.1 mammalian expression vector (Invitrogen) with a V5 and His_6 tag at the COOH terminus of TGFBI. Deletion and point mutation mutants of TGFBI and periostin were generated in using conventional PCR methods and the QuikChange site-directed mutagenesis kit (Stratagene), following the manufacturer's instructions. The sequences of all constructs were verified by direct sequencing.

Antibodies—The primary antibodies used in this study were as follows: mouse monoclonal anti-TGFBI antibody, a kind gift from Dr. In-San Kim (Kyoung Pook University, Korea) (48); goat polyclonal anti-TGFBI (R&D Systems); rabbit polyclonal anti-periostin (ab14041; Abcam); mouse monoclonal anti-V5 (Invitrogen); goat polyclonal anti-periostin (C-20), anti-actin (A-19), mouse monoclonal anti-tenascin-C (300-3), anti-GFP(B-2), mouse monoclonal anti-Myc(9E10), rabbit polyclonal anti-collagen type VI, and TGN38 (Santa Cruz Biotechnology, Inc., Santa Cruz, CA); mouse monoclonal anti-Lamp2 (H5C6; BD Pharminogen); horseradish peroxidase-conjugated anti-mouse (GE Healthcare); horseradish peroxidase-conjugated anti-rabbit (GE Healthcare); and anti-goat IgG (Santa Cruz Biotechnology, Inc.). The secondary antibodies used for immunofluorescence were as follows: goat anti-mouse or goat anti-rabbit conjugated to Alex Fluor 488 or 594 (Invitrogen).

Cell Culture and Transfections—HeLa, COS-7, HEK293, and human corneal fibroblast (HCF) cell lines were grown in Dulbecco's modified Eagle's medium (Invitrogen) supplemented with 2 mM L-glutamine, 100 units/ml penicillin, 100 μg/ml streptomycin, and 10% (w/v) fetal bovine serum (Invitrogen) at 37 °C in a 5% CO_2 incubator. The human corneal epithelial (HCE) cell line was grown in Dulbecco's modified Eagle's medium and F-12 (1:1) media supplemented with 2 mM L-glutamine, 100 units/ml penicillin, 100 μg/ml streptomycin, 10% (w/v) fetal bovine serum, 10 ng/ml recombinant human epidermal growth factor (R&D Systems) at 37 °C in a 5% CO_2 incubator. Human corneal epithelial and fibroblast cell lines were a kind gift from Dr. Shigeru Kinoshita (Kyoto Prefectural University of Medicine, Japan) and Dr. James V. Jester (University of California, Irvine, CA). Primary corneal fibroblasts were cultured from corneal buttons obtained from a 60-year-old control and a 27-year-old homozygous GCD II patient during penetrating keratoplasty. The endothelial and epithelial layers were removed from the corneas, and stroma was used as explants to initiate corneal fibroblast cultures. The cells were maintained in Dulbecco's modified Eagle's medium supplemented with 2 mM L-glutamine, 100 units/ml penicillin, 100 μg/ml streptomycin, and 10% (w/v) fetal bovine serum at 37 °C in a 5% CO_2 incubator. Donor confidentiality was maintained according to the Declaration of Helsinki and was approved by the Severance Hospital IRB Committee (CR04124). Transfections were performed using GeneJammer (Stratagene) according to the manufacturer's instructions, analyses were conducted 24 h post-transfection, and immunoprecipitations were carried out as described previously (49).

Western Blot—Cells were washed with PBS, and extracts were obtained by passing the suspension through a 26-gauge

needle in ice-cold lysis buffer (50 mM Tris-HCl, pH 7.4, 150 mM NaCl, 1% Nonidet P-40, 0.1% Triton X-100 supplemented with protease inhibitor mixtures (Applied Biological Materials Inc.)). Soluble supernatants were analyzed by SDS-PAGE under reducing conditions and transferred to nitrocellulose membranes (Millipore). The membrane was then blocked with 5% skim milk (Difco) in 1× TBST buffers (20 mM Tris-HCl, 137 mM NaCl, pH 7.6, 0.1% Tween 20) and incubated with the indicated antibodies. The SuperSignal West Pico chemiluminescent substrate Kit (Thermo Scientific) was used for protein detection. The band intensities were quantified using the ImageJ program (version 1.38).

Human Corneal Epithelium Protein Extracts—Normal human corneal epithelial cells were obtained by scraping the epithelial layer during photorefractive keratectomy. Patient corneal epithelial cells from a GCD II patient were obtained by scraping the epithelial layer during deep lamellar corneal transplantation. After scraping the corneal surface using a blunt blade, samples were immediately placed into ice-cold lysis buffer, and proteins were extracted.

His Tag Pull-down Assays—For His tag pull-down assays, COOH-terminal His-tagged wild type of TGFBI was purified as described previously (25), and NH_2-terminal His-tagged periostin was purchased from BioVendor. Twenty micrograms of His-tagged recombinant TGFBI or periostin was immobilized on nickel-agarose resin (Applied Biological Materials) and incubated overnight at 4 °C with 500 μg of HCF cell lysates. Bound proteins were resolved by SDS-PAGE and detected by Western blotting with the indicated antibodies.

Immunofluorescence Microscopy and Immunohistochemistry—For immunofluorescence microscopy, cells were grown on coverslips, fixed in cold methanol/acetone (1:1, v/v) for 10 min at −20 °C, and blocked with 2% bovine serum albumin for 30 min. Cells were incubated with primary antibodies in 2% bovine serum albumin for 1 h at room temperature. Cells were washed with PBS and subsequently incubated with secondary antibodies in 2% bovine serum albumin for 1 h at room temperature. After washing with PBS, cells were mounted using Vectashield (Vector Laboratories, Inc.). Images were acquired using a TCS SP5 confocal microscope (Leica).

For immunohistochemistry analyses, corneas from normal human, R124H mutated heterozygous and homozygous GCD II patients were fixed in 10% neutral-buffered formalin and embedded in paraffin. The paraffin-embedded samples were sectioned on a microtome at a thickness of 5 μm, mounted on slide glasses, deparaffinized in xylene, and rehydrated in ethanol. The sections were incubated in 0.3% H_2O_2 for 30 min and blocked with 2.5% normal horse serum for 20 min. The sections were then incubated with normal rabbit IgG serum and/or rabbit polyclonal anti-periostin antibody (1:500, v/v) in 2.5% normal horse serum and 0.1% bovine serum albumin for 1 h at room temperature. The sections were washed with PBS and incubated in ImPress universal reagent (Vector Laboratories) for 30 min. After washing with PBS for 5 min, the sections were incubated with DAB solution and visualized according to the manufacturer's instructions (Vector Laboratories). Sections were washed with PBS three times and mounted using Vectashield (Vector Laboratories). Masson's trichrome stains were used to confirm the mutated TGFBI deposits in the corneal stroma. Images were acquired using a BX 40 light microscope (Olympus).

RESULTS

Periostin Is Expressed in Cornea-derived Cell Lines and Corneal Tissues—Despite the fact that TGFBI and periostin share several similarities in structure and expression patterns (Fig. 1*A*) (15, 33), little is known about the roles of periostin in corneal tissues. To examine the expression of periostin in cornea and cornea-derived cells, we first performed Western blot analysis with specific anti-periostin antibodies (C-20 and ab14041) (Fig. 1*B*). Western blot analysis revealed expression of periostin in all of the tested cells and tissues, including COS-7, HeLa, HEK293, and HCF (40); primary cultured corneal fibroblast from normal human (NPCF) and HCE cell lines (41); and normal human corneal epithelium (Fig. 1*B*, *top*, *lanes 1–7*). In HeLa, COS-7, HEK293, HCF, and NPCF, endogenous periostin was detected primarily as a single band that migrated with an apparent molecular mass of ~85 kDa, consistent with the predicted molecular weight (Fig. 1*B*, *lanes 1–5*). A second high molecular mass band of ~170 kDa was observed in some cell lines. This band may represent the previously reported covalently linked periostin multimer (42) or perhaps some other covalent posttranslational modification. However, in HCE and corneal epithelium, periostin was detected as a single band of ~60 kDa (Fig. 1*B*, *top*, *lanes 6* and *7*). The C-20 anti-periostin antibody was raised against a COOH-terminal periostin peptide (amino acids 725–775), and preabsorption with a periostin peptide completely abolished the immunoreactivity of anti-periostin antibody (C-20), confirming the specificity of this antibody (Fig. 1*B*, *second panel*). To further determine the identity of the periostin-immunoreactive band, we performed additional Western blot analyses using an independent anti-periostin antibody generated against a separate epitope (ab14041, amino acids 22–669) and found that this antibody also recognized the ~60 kDa band in human corneal epithelium (supplemental Fig. 1). Together, these results suggest that periostin is expressed in cornea-derived fibroblast and epithelial cell lines as well as in corneal epithelium. In addition, the detection of a form of periostin of reduced molecular weight with two anti-periostin antibodies that recognize separate periostin epitopes raises the possibility of cell type-specific proteolytic processing of periostin or cell type-specific periostin splice variants.

Periostin Interacts with TGFBI in Vivo and in Vitro—Periostin has previously been shown to form dimers (42), and given the structural similarity between periostin and TGFBI, we next sought to determine whether the two proteins interact. We first performed pull-down assays using immobilized His-tagged TGFBI or periostin with HCF cell lysates. Bound proteins were separated by SDS-PAGE and visualized by Western blotting. As shown in Fig. 2A, His-tagged TGFBI efficiently pulled down endogenous periostin from HFC cell lysates (Fig. 2*A*). Consistent with previous reports (19, 23, 24), we found that collagen VI was readily pulled down from HFC cell lysates by His-tagged recombinant TGFBI (Fig. 2*A*).

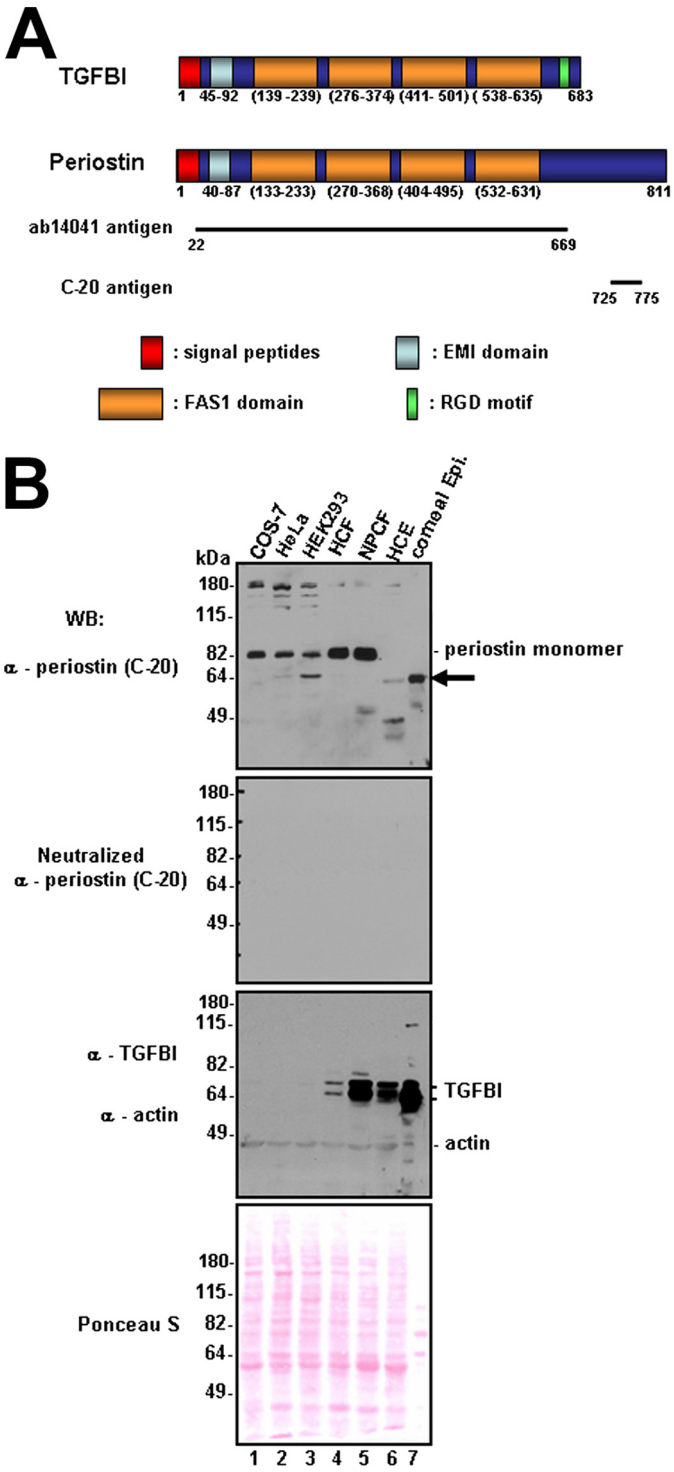

FIGURE 1. **Periostin is expressed in human cornea.** *A*, schematic representation of TGFBI and periostin. TGFBI and periostin contain NH_2-terminal signal peptides, followed by a cysteine-rich EMI domain and four tandem FAS1 domains. TGFBI also contains a COOH-terminal RGD motif that is not present in periostin, which instead contains a COOH-terminal hydrophilic region. The following domains of TGFBI and periostin are indicated: EMI, FAS1, fasciclin 1, and Arg-Gly-Asp (*RGD*). Antigenic regions of antibodies used in this study (ab14041 and C-20) are represented by *black lines*. *B*, cell and tissue lysates were separated by SDS-PAGE and Western blotted using the indicated antibodies. Anti-periostin antibody (C-20) recognizes an ~85-kDa protein in several cell lines and corneal fibroblast cell lines. In contrast, anti-periostin antibody recognizes a ~60-kDa form in corneal epithelial cell lines and corneal epithelium tissues (*top*, *black arrow*). The specificity of periostin antibody (C-20) was confirmed by preabsorption with 10 μg of C-20 antigen peptide (*second panel*). *WB*, Western blot.

In addition, His-tagged TGFBI did not pull down the cytoskeletal protein actin, confirming the specificity of this experiment. In the reciprocal experiment, we found that His-tagged periostin efficiently pulled down endogenous TGFBI, but not actin or collagen VI. These *in vitro* binding studies indicate that periostin is able to interact with TGFBI. These results also show that periostin does not interact with the TGFBI-binding partner collagen VI (Fig. 2*B*), indicating that despite the large degree of sequence similarity, periostin and TGFBI are not interchangeable.

To verify that the periostin-TGFBI interaction occurs *in vivo*, we performed co-immunoprecipitation experiments using antibodies specific for periostin and TGFBI. As shown in Fig. 2*C*, anti-TGFBI antibodies, but not the IgG control, efficiently co-immunoprecipitated endogenous periostin from HCF cell lysates. Furthermore, anti-periostin antibodies specifically co-immunoprecipitated endogenous TGFBI from HCF cell lysates (Fig. 2*D*, *lane 3*). Taken together, the pull-down assays and co-immunoprecipitation experiments demonstrate that periostin interacts with TGFBI *in vitro* and *in vivo*.

The Periostin and TGFBI Interaction Is Mediated by the Amino-terminal, Cysteine-rich EMI Domain—To map the binding sites mediating the interaction between periostin and TGFBI, we generated a series of COOH-terminally V5/His-tagged TGFBI deletion mutants and COOH-terminally GFP-tagged periostin deletion mutants (Fig. 3, *A* and *C*) and performed coimmunoprecipitation analyses. As shown in Fig. 3*B*, all of the NH_2-terminal deletion mutants of TGFBI (ΔN1–ΔN4) abolished the interaction with GFP-tagged wild type of periostin (*lanes 2–5*). In contrast, the full-length and ΔN5 deletion mutant of TGFBI, in which the first and second FAS1 domain regions are deleted, both efficiently precipitated GFP-tagged full-length periostin (Fig. 3*B*, *lanes 1* and *6*). These results suggest that the NH_2-terminal, cysteine-rich EMI domain of TGFBI is critical for the interaction with periostin. In addition, using NH_2-terminal deletions of periostin, we found that the NH_2-terminal, cysteine-rich EMI domain of periostin is critically required for the interaction with TGFBI. As shown in Fig. 3, GFP-tagged full-length periostin efficiently coimmunoprecipitated V5/His-tagged full-length TGFBI (Fig. 3*D*, *lane 1*). In contrast, NH_2-terminal deletion mutants of periostin (ΔN2–ΔN5) completely abolished the interaction with V5/His-tagged full-length TGFBI (Fig. 3*D*, *lanes 2–6*). To test whether the predicted binding region (EMI domain) of TGFBI and periostin are responsible for the interactions, we generated the COOH-terminally V5/His-tagged TGFBI-EMI and COOH-terminally GFP-tagged periostin-EMI constructs (Fig. 3, *E* and *G*) and performed coimmunoprecipitation using the indicated antibodies. The results confirmed that the NH_2-terminal EMI domains are sufficient for the interactions between TGFBI and periostin (Fig. 3, *F* and *H*). Taken together, these deletion mapping analyses provide evidence supporting a model in which the binding between TGFBI and periostin is mediated via NH_2-terminal, cysteine-rich EMI domains in both TGFBI and periostin (Fig. 3*I*).

Periostin Colocalizes with TGFBI in the trans-Golgi Network—To provide further evidence for an *in vivo* association of periostin with TGFBI, we employed immunofluorescence confocal

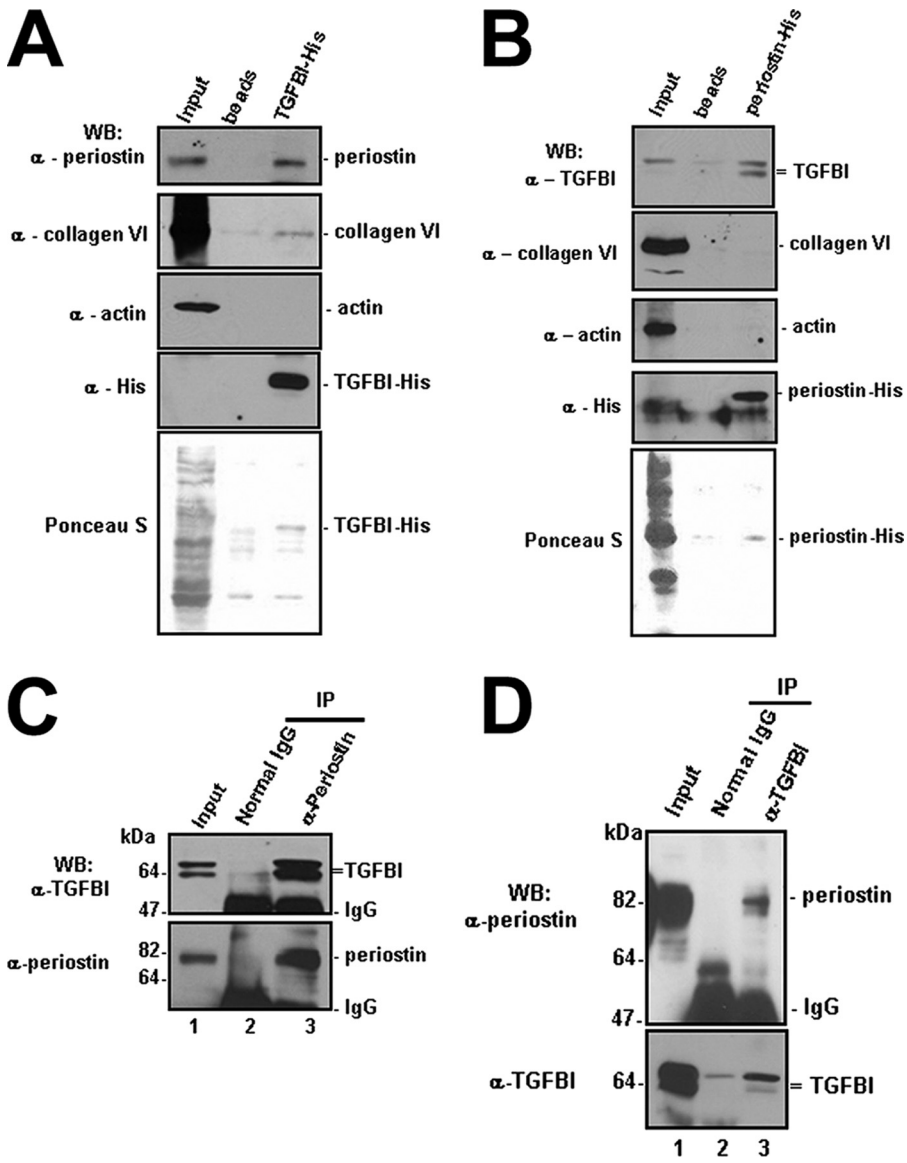

FIGURE 2. **Periostin specifically interacts with TGFBI.** *A* and *B*, *in vitro* His pull-down assays were performed by incubation of nickel-nitrilotriacetic acid beads alone, immobilized His-tagged recombinant TGFBI, or immobilized His-tagged periostin with HCF cell lysates. Bound periostin and TGFBI were detected by Western blotting using specific antibodies (*first panel*). Collagen VI and actin were used for positive and negative controls using specific antibodies as indicated (*second* and *third panels*). Immobilized His-recombinant TGFBI and periostin were detected using anti-His antibody (*fourth panel*). *C* and *D*, co-immunoprecipitation of endogenous periostin and TGFBI in HCF cell lysates. Endogenous TGFBI or periostin was immunoprecipitated from HCF cell lysates with anti-TGFBI or anti-periostin antibodies, respectively, followed by Western blotting for periostin or TGFBI (*lane 3*). Normal mouse or rabbit IgG was used as negative control (*lane 2*). *WB*, Western blot; *IP*, immunoprecipitation.

microscopy to examine the subcellular localization of periostin and TGFBI. As shown in Fig. 4*A*, GFP-tagged periostin expressed in COS-7 cells localizes to a perinuclear region (*a* and *d*) that colocalizes with TGN38, a *trans*-Golgi network (TGN) marker (*a–c*). GFP-tagged periostin fluorescence did not colocalize with the late endosome and lysosome marker, Lamp2 (*d–f*). The COOH-terminally V5/His-tagged full-length TGFBI showed a similar staining pattern that also colocalized with TGN38 (*g–i*) but not Lamp2 (*j–l*). Immunostaining of COS-7 cells co-expressing GFP-tagged full-length periostin and V5/His-tagged TGFBI revealed clear overlapping subcellular distributions (*m–o*), indicating that periostin and TGFBI colocalize in COS-7 cells. To determine the subcellular localizations of endogenous periostin and TGFBI, we employed antibodies specific for periostin and TGFBI in HCF cells. Consistent with the above results, we found that endogenous TGFBI and periostin both colocalized with TGN38 immunostaining (Fig. 4*B*, *a–f*). In addition, endogenous periostin and TGFBI immunostaining showed a substantial amount of overlap (Fig. 4*B*, *g–i*). Taken together, these results demonstrate that endogenous periostin and TGFBI colocalize in the *trans*-Golgi network.

The GCD II-associated R124H Mutant TGFBI Impairs Binding of Periostin—Our biochemical and immunofluorescence microscopy results strongly suggest that periostin and TGFBI cooperated in the same pathways in the cells. To further our understanding of the pathophysiology of 5q31-linked corneal dystrophies, we next examined the effects of 5q31-linked corneal dystrophy mutations in TGFBI on its interaction with periostin. COS-7 cells co-expressing GFP-tagged periostin and V5/His-tagged wild type and mutant TGFBI were subjected to immunoprecipitation with GFP antibodies. Several corneal dystrophy-associated TGFBI mutants were examined, including R124H (GCD II), R124C (lattice corneal dystrophy I), R124L (Reis-Bucklers corneal dystrophy), R555W (GCD I), and R555Q (Thiel-Behnke corneal dystrophy). Interestingly, we found that R124H mutant TGFBI significantly decreased binding of periostin (*lane 2*) compared with wild type TGFBI as well as other TGFBI mutants (Fig. 5, *lanes 1* and *3–6*). Quantification of three independent experiments confirmed that the R124H mutation in TGFBI disrupts the interaction between TGFBI and periostin (Fig. 5*B*). The R124H mutation causes granular corneal dystrophy type II. To further examine whether the interaction between TGFBI and periostin is indeed disrupted by the R124H mutation, we performed coimmunoprecipitation experiments using primary cultured corneal fibroblasts from normal human control and homozygous R124H GCD II patients. Consistent with our results, endogenous wild type of TGFBI coprecipitated with an anti-periostin-specific antibody (Fig. 5*C*, *lane 2*). In contrast, binding of the R124H

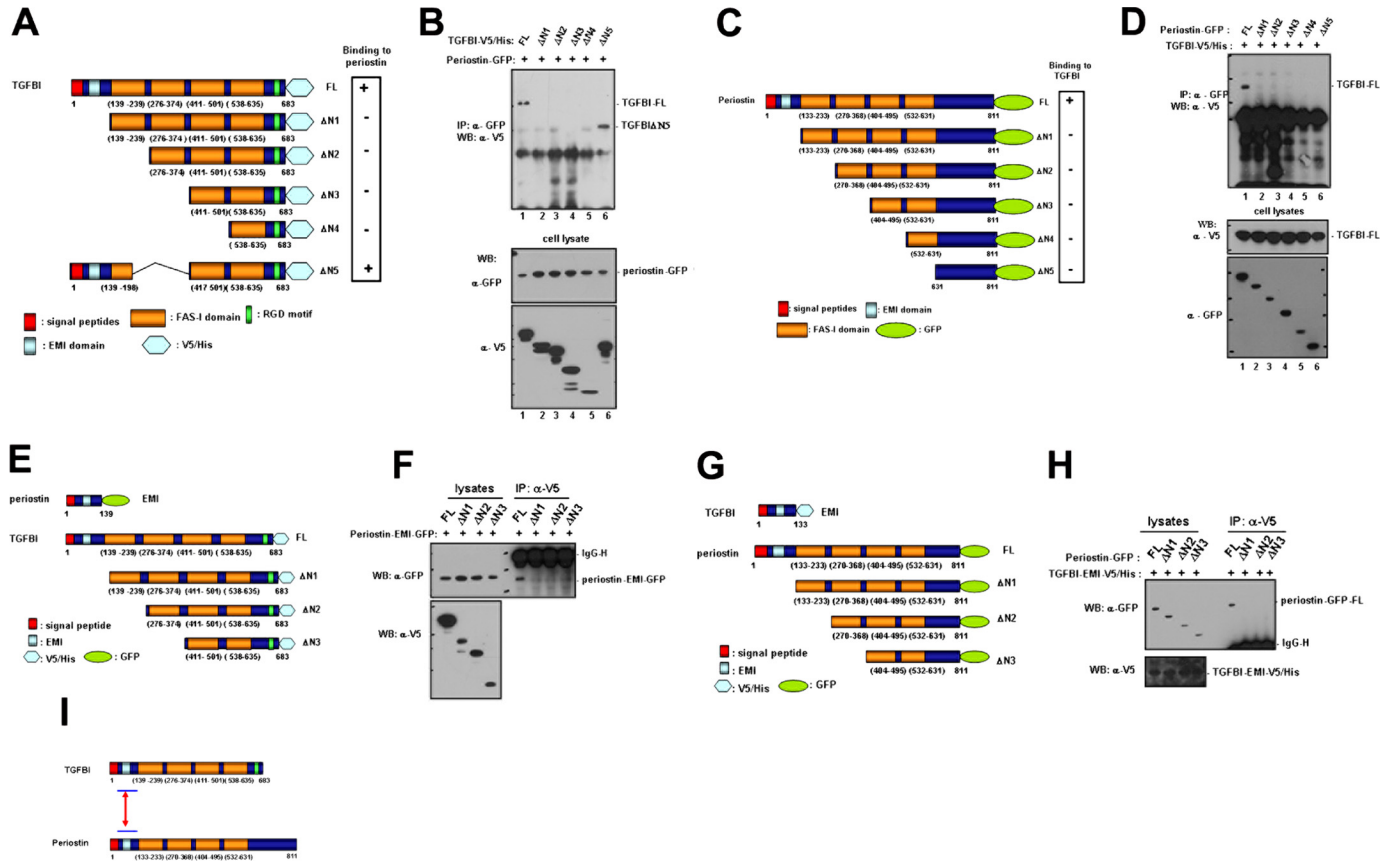

FIGURE 3. **Identification of periostin and TGFBI binding sites by deletion analyses.** *A*, *C*, *E*, and *G*, schematic representation of human TGFBI and periostin full-length and deletion constructs used in this study. *B*, *D*, *F*, and *H*, the TGFBI-periostin interaction is mediated by the EMI domain. COS-7 cells coexpressing the indicated V5/His-tagged wild type or deletion mutants of TGFBI with GFP-tagged wild type or deletion mutants of periostin were immunoprecipitated with anti-V5 or anti-GFP antibodies, followed by Western blotting with the indicated antibodies. *IP*, immunoprecipitation; *WB*, Western blot. *I*, model illustrating the identified binding sites of TGFBI and periostin.

mutant TGFBI to periostin is dramatically reduced in corneal fibroblasts from GCD II patients (Fig. 5*C*, *lane 4*). Together, these results demonstrate that the R124H mutation in TGFBI, which is responsible for GCD II, impairs binding of periostin, suggesting the possibility that impaired binding of periostin may be one contributing factor to the pathophysiology of GCD II.

To test whether 5q31-linked corneal dystrophy mutations in TGFBI affect its secretion, we analyzed both the intracellular TGFBI and the TGFBI secreted into the cell media from HEK293 cells expressing V5/His-tagged wild type and mutant TGFBI by Western blotting. As shown, we did not find any significant differences in the secretion of wild type and mutant TGFBI (Fig. 5*D*). Experiments in which corneal fibroblasts cultured from normal human and GCD II patients were employed yielded similar data (data not shown), indicating that 5q31-linked corneal dystrophy mutations in TGFBI do not significantly affect its secretion.

The GCD II-associated R124H Mutant TGFBI Mislocalizes to Lysosomes—Since the R124H mutation of TGFBI seriously impaired the interaction with periostin, we performed immunofluorescence confocal microscopic analyses to examine the subcellular localization of R124H mutant TGFBI. Consistent with the above result in immunofluorescence analysis, V5/His-tagged wild type TGFBI showed a typical perinuclear localization pattern, which colocalized with the TGN38 immunostaining (Fig. 6*A*, *a–c*) but not Lamp2 immunostaining (Fig. 6*B*, *a–c*). In contrast, the V5/His-tagged R124H mutant TGFBI showed significant changes in subcellular localization. In addition to a slight overlap with TGN immunostaining, the R124H mutant TGFBI was found to be predominantly associated with cytosolic vesicles that largely colocalized with Lamp2-immunoreactive puncta (Fig. 6*B*, *d–f*). Quantification of the subcellular distribution of the R124H mutant of TGFBI revealed a significant shift from TGN to late endosomes and lysosomes when compared with the distribution of wild type TGFBI (Fig. 6*C*). To confirm these results in the endogenous state, we examined the distribution of endogenous TGFBI in cultured corneal fibroblasts from normal human control and homozygous R124H GCD II patients. As shown in Fig. 6*D*, we found that the number of TGFBI-positive cytosolic vesicles was increased in cultured corneal fibroblasts from the GCD II patient (*bottom*) when compared with the more typical TGN localization of wild type TGFBI in cultured corneal fibroblasts from the normal control patient (*top*). Furthermore, the degree of overlap between TGFBI and periostin was reduced in GCD II cultured corneal fibroblasts (Fig. 6*D*). Interestingly, Western blot analyses of lysates prepared from normal and GCD II patient corneal fibroblasts indicate an increase in the levels of periostin but not TGFBI (data not shown). Together, these results indicate that

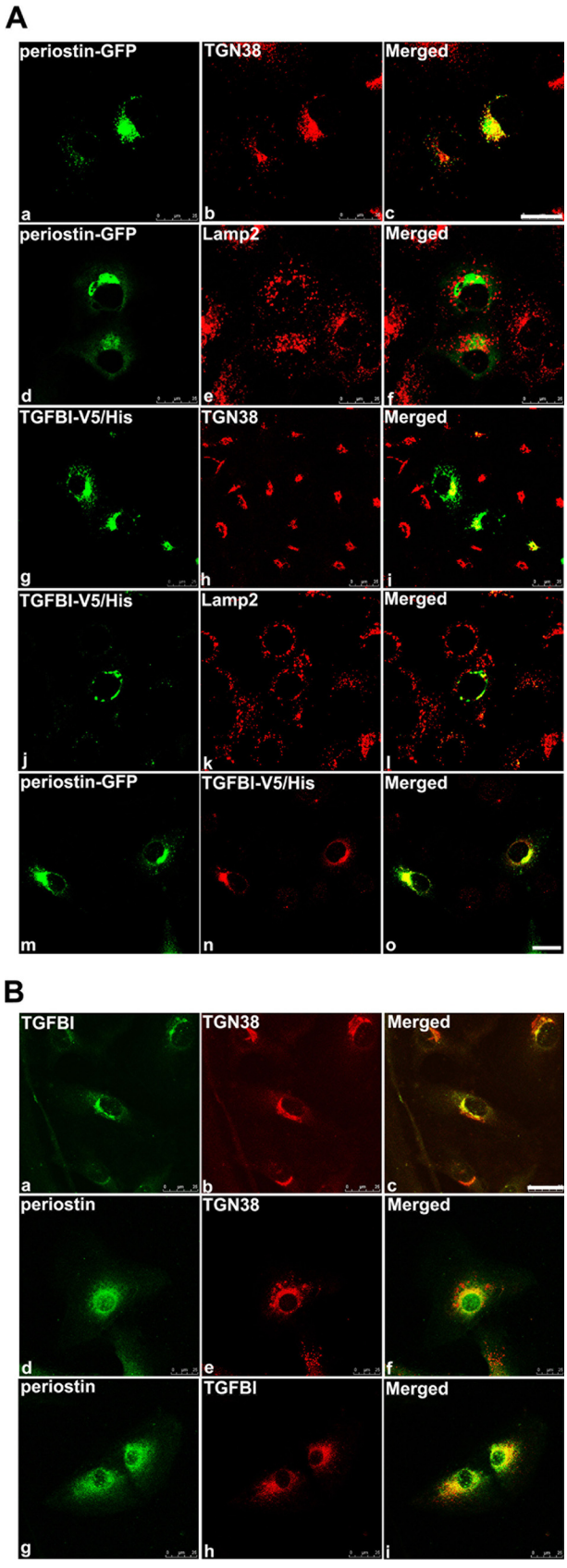

FIGURE 4. **Periostin TGFBI colocalize in the trans-Golgi network.** *A*, COS-7 cells expressing the GFP-tagged periostin were immunostained with antibodies against TGN38 (*a–c*) or Lamp2 (*d–f*). COS-7 cells expressing the V5/His-tagged TGFBI were immunostained with antibodies against V5 and TGN38 (*g–i*) or Lamp2 (*j–l*). GFP-tagged periostin and V5/His-tagged TGFBI were coexpressed into COS-7 cells and immunostained with antibodies against V5 (*m–o*). GFP-periostin was directly visualized by GFP fluorescence. *B*, HCF cell lines were immunostained with antibodies against periostin and TGN38 (*a–c*), TGFBI and TGN38 (*d–f*), or periostin and TGFBI (*g–i*). *Scale bars*, 25 μm.

the R124H mutation disrupts the normal TGFBI localization, resulting in the abnormal presence of a lysosomal pool of R124H mutant TGFBI.

Periostin Accumulates in R124H Mutant TGFBI Deposits in GCD II Corneal Tissues—The biochemical and cell biological analyses in our studies strongly suggest the possibility that periostin plays a role in the pathogenesis of GCD II. Therefore, we next examined the distribution of periostin in control as well as heterozygous and homozygous R124H GCD II patient corneal tissues. As expected, Masson's trichrome staining revealed the presence of large deposits in the corneal stroma from both heterozygous and homozygous R124H GCD II but not the control tissues (Fig. 7*A*). Immunostaining with anti-TGFBI (Fig. 7*A*, *g*) and anti-periostin (Fig. 7*A*, *j*) antibodies showed strong immunoreactivity in corneal epithelium and a small amount of diffuse staining within the corneal stroma in the normal human control corneal tissue. In contrast, in the corneas from heterozygous and homozygous R124H GCD II patients, strong immunoreactivity was detected in the deposits in the corneal stroma by both the TGFBI-specific (Fig. 7*A*, *h* and *i*) and periostin-specific antibodies (Fig. 7*A*, *k* and *l*). Importantly, the deposits were not stained by the normal rabbit IgG control (Fig. 7*A*, *d–f*), indicating the specificity of these staining patterns.

These findings indicate that periostin accumulates in mutant TGFBI corneal deposits and raise the possibility that periostin may co-aggregate with mutant TGFBI in GCD II patients. To examine this possibility, we performed Western blotting analyses of protein extracts from scraped corneal epithelial layers of normal human control and homozygous R124H GCD II patients. As shown in Fig. 7*B*, we found that the TGFBI antibody recognized monomeric TGFBI in control and GCD II patients. Moreover, there was an increase in the total amount of TGFBI protein and the appearance of high molecular weight forms of TGFBI in the GCD II patient tissue (Fig. 7*B*, *first panel*). We also found that the anti-periostin antibody strongly reacted with high molecular weight forms of periostin in the samples from the GCD II patient that were absent in control tissues (Fig. 7*B*, *second panel*). These TGFBI and periostin high molecular weight bands were completely absent in the control samples even when 20 times more sample was loaded (data not shown), indicating that these bands are specific to the disease state. In contrast to TGFBI and periostin, other extracellular matrix proteins previously reported to interact with TGFBI and periostin, such as fibronectin and tenascin C, did not show differential levels in normal or GCD II patient samples (Fig. 7*B*, *panels 3–5*). In addition, reverse transcription-PCR analyses of the TGFBI and periostin transcripts indicate that there is little change in the mRNA levels in normal and disease tissues (data not shown), suggesting that the increase in protein levels is due to accumulation within the extracellular deposits. Taken together, these results strongly indicate the possibility that periostin co-aggregates in mutant TGFBI corneal deposits and raise

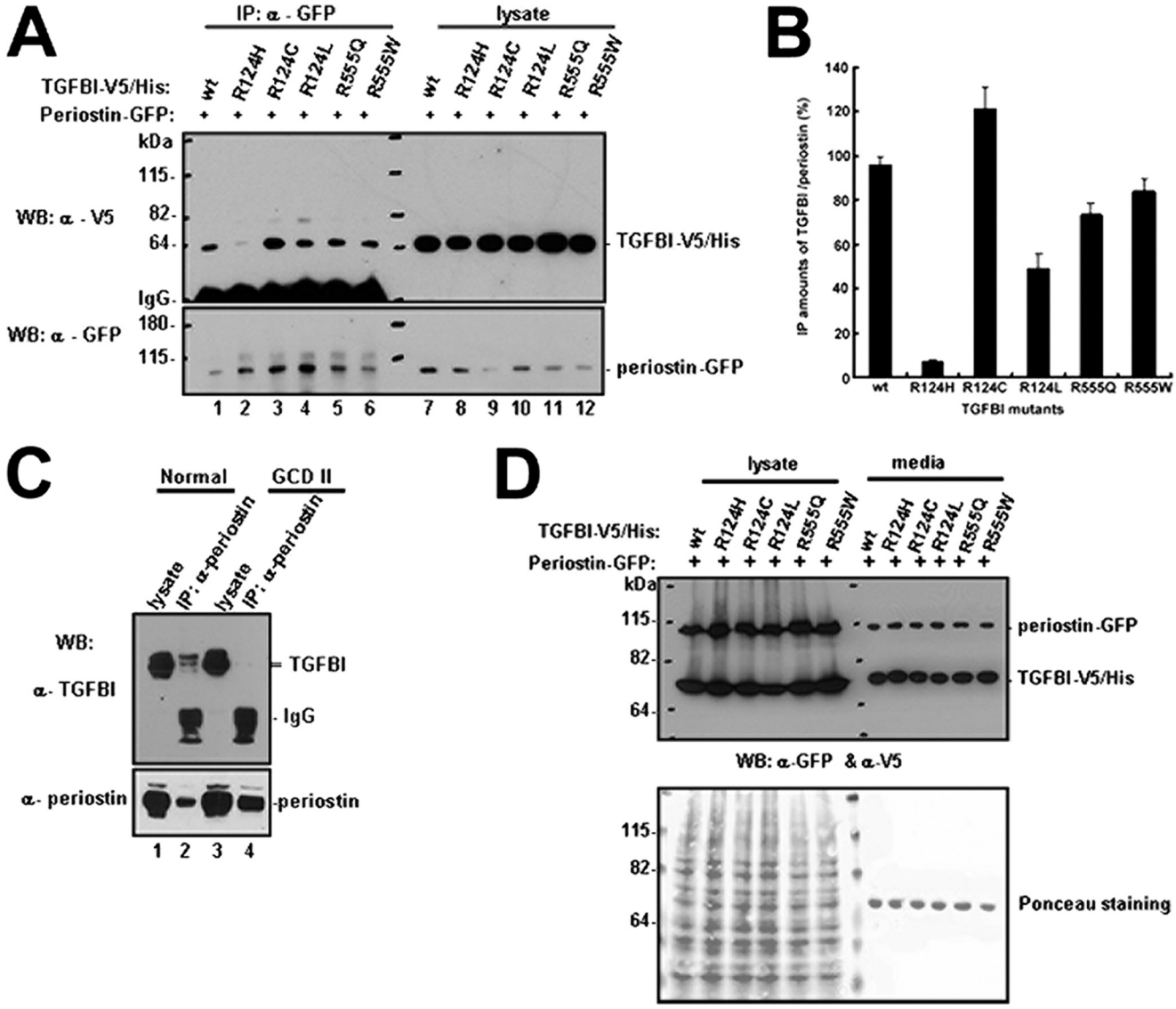

FIGURE 5. **GCD type II-associated R124H mutant TGFBI disrupts the interaction with periostin.** *A*, COS-7 cells coexpressing GFP-tagged periostin and V5/His-tagged wild type and 5q31-linked corneal dystrophies-associated mutant forms of TGFBI were subjected to immunoprecipitation with anti-GFP antibody, followed by Western blotting with anti-V5 and anti-GFP antibodies. *B*, quantification of the precipitated amounts of mutant TGFBI. Amounts of precipitated V5/His-tagged TGFBI were normalized to the amount of precipitated GFP-tagged periostin. Data represent mean ± S.E. from three independent immunoprecipitation experiments. *C*, primary cultured corneal fibroblasts from a normal human patient and a GCD II patient bearing homozygous R124H mutations in TGFBI were subjected to immunoprecipitation with anti-periostin antibody, followed by Western blotting with anti-TGFBI and anti-periostin antibodies. *D*, cell lysate or cell media from COS-7 cells coexpressing GFP-tagged periostin with V5/His-tagged wild type and 5q31-linked corneal dystrophy-associated mutant forms of TGFBI were analyzed by Western blotting with anti-V5 and anti-GFP antibodies. *WB*, Western blot; *IP*, immunoprecipitation.

the possibility that periostin is involved in the pathogenesis of 5q31-linked corneal dystrophies.

DISCUSSION

Despite many recent studies on TGFBI in 5q31-linked corneal dystrophies, the precise molecular mechanisms by which mutations in TGFBI cause the characteristic disease phenotypes remain poorly understood. In addition, although there is a high degree of overall similarity between TGFBI and periostin, periostin has not been previously implicated in corneal biology or in the pathogenesis of 5q31-linked corneal dystrophies. In this study, we show that periostin is expressed by human cornea-derived cells, and we identify a specific interaction between TGFBI and periostin. Moreover, our results demonstrate that the R124H mutation in TGFBI impairs the interaction with periostin and results in the mislocalization of a portion of TGFBI to lysosomes. Finally, we find that periostin accumulates in deposits of aggregated mutant TGFBI in the corneal stroma of GCD II patients.

Periostin was originally identified as a ~90-kDa secreted protein in murine osteoblasts and originally termed OSF-2 (osteoblast-specific factor-2) (31). Later, it was renamed periostin due to its expression in the periosteum and periodontal ligament (33). Although it has been shown that periostin is widely expressed in many different cell types, including connective, bone, periodontal ligament, and several types of cancer (31–34), its expression in corneal cells and tissues has not been

reported. Using two anti-periostin antibodies that recognize distinct periostin epitopes, we show that periostin is expressed by cornea-derived fibroblast and epithelial cells, suggesting the possibility that periostin plays a role in corneal cells. Interestingly, despite the predicted molecular mass of periostin, which is ~90 kDa, it was detected as a ~60-kDa species in HCE cells and human corneal epithelium by two different periostin-specific antibodies, C-20 and ab14041. The specificity of this lower band was confirmed by preabsorption experiments employing a periostin peptide. A lower molecular weight form of periostin has previously been reported by Kern *et al.* (44) in chick developing heart using a periostin antibody recognizing a more NH_2-terminal epitope, providing further support for the identity of this anti-periostin-reactive band. Potential splicing events could result in this lower molecular weight periostin species. However, although it was previously reported that several alternative splicing variants of periostin exist (32, 39), all of the spliced forms are ~80–90 kDa (32, 38, 39). A second possibility is that the lower molecular weight form of periostin represents the product of proteolytic processing. Thus, it may be that periostin undergoes a proteolytic processing event that is specific to corneal tissues. Our findings indicate that a novel, lower molecular weight form of periostin exists in human corneal epithelium. Further studies will be important to understand the precise molecular events that give rise to this lower molecular weight form of periostin.

Our *in vitro* and *in vivo* biochemical analyses revealed a specific interaction between exogenously expressed TGFBI and periostin in COS-7 cells and endogenous TGFBI and periostin in human corneal fibroblasts. These results raise the possibility that TGFBI and periostin function in the same regulatory pathways in human cornea. Indeed, previous reports have shown that both TGFBI and periostin function as cellular adhesion molecules and are involved in the promotion of cancer metastasis (35, 45). Our coimmunoprecipitation experiments using deletion mutants of TGFBI and periostin revealed that TGFBI and periostin association is mediated by the NH_2-terminal, cysteine-rich EMI domain of both TGFBI and periostin (Fig. 3, *A–I*). The EMI domain was first named after its presence in proteins of the EMILIN family and suggested to be the protein-protein interaction motif (17, 33, 46). Interestingly, previous reports have shown that the interaction of periostin and the ECM proteins fibronectin, tenascin C, and collagen V is mediated via the FAS1 domain (39). Thus, the interaction of TGFBI and periostin via the EMI domain would potentially leave the FAS1 domain free for interaction with other binding partners, suggesting that the TGFBI-periostin interaction would not necessarily preclude simultaneous binding to effector proteins. We further found that the deletion of the FAS1 domain had no effect on the TGFBI-periostin interaction, and the expression of the EMI domain alone was sufficient to recapitulate the interaction between the two molecules. In addition, we noted that despite the high degree of similarity between TGFBI and periostin, periostin does not interact with the TGFBI-interacting protein collagen VI (Fig. 2*B*). These results are intriguing and provide evidence that, although highly similar, TGFBI and periostin are not interchangeable.

Both TGFBI and periostin contain NH_2-terminal signal sequences, which are expected to be necessary for their cotranslational insertion into the endoplasmic reticulum, the port of entry into the cellular secretory system. After folding within the endoplasmic reticulum, proteins destined for secretion are transported to the Golgi apparatus prior to their secretion. Our immunofluorescence microscopic analyses are consistent with this folding and processing pathway and show that endogenous TGFBI and periostin colocalize in the TGN. In addition, we show that both proteins are efficiently secreted from cells and that corneal dystrophy-associated mutations in TGFBI have no effect on its secretion. In fact, the levels of mutant TGFBI secretion were indistinguishable from wild type TGFBI, indicating a failure in the ER quality control mechanisms to recognize and degrade these mutant proteins. It is possible that these mutations do not result in gross misfolding of TGFBI, which would be expected to expose buried hydrophobic regions that would allow quality control proteins to recognize and dispose of them. Instead, these mutations may disrupt local TGFBI surfaces that affect interactions with critical binding partners, such as periostin.

Our findings indicate that several corneal dystrophy-associated mutations in TGFBI display reduced binding of periostin, with the R124H mutation causing the most severe impairment in periostin binding. We further confirmed this result using primary cultured corneal fibroblasts from a GCD II patient bearing homozygous R124H mutations. These results clearly show that the interaction between periostin and TGFBI was severely reduced by the R124H mutation in TGFBI (Fig. 5*C*, *lane 4*), providing the first evidence implicating periostin in GCD II. Our immunofluorescence analyses provide further support for the importance of the Arg^{124} residue. We found that in COS-7 cells expressing R124H mutant TGFBI, a large portion was aberrantly localized to Lamp2-immunoreactive late endosomes and lysosomes. We also found that R124H mutant TGFBI showed a similar redistribution in primary cultured corneal fibroblasts from a GCD II patient bearing homozygous R124H mutations. The precise reason for this redistribution is currently unclear and will require further study. It is possible that a portion of the R124H mutant TGFBI is recognized as misfolded and is degraded via the lysosome through a specialized autophagic process termed ER-phagy. Indeed, this has been shown to occur for the Z-variant of α1-antitrypsin, which causes severe misfolding and aggregation in the ER (47). However, our analyses indicate that the R124H mutant is secreted normally, and a second possibility is that this mutant is endocytosed and trafficked to the lysosome for degradation. Further studies will be necessary to determine the molecular basis underlying the lysosomal localization of the R124H mutant TGFBI. It is interesting to note that the Arg^{124} residue is found within the initial NH_2-terminal segment of TGFBI near the EMI domain, which mediates an association with periostin. Mutations to the Arg^{555} residue had no affect on the association with periostin, probably because the Arg^{555} residue is within the fourth FAS1 domain and is spatially separated from the periostin-binding site. Interestingly, R124L and R124C also had no effect on peri-

ostin binding. One possibility is that the R124H mutation induces more severe structural changes in the NH_2 terminus than the other TGFBI mutations and that these changes affect periostin binding. Previous structural analyses of the FAS1 domain indicate that the Arg^{124} residue would be solvent-exposed, and distinct amino acid substitutions could have very different effects on TGFBI intermolecular contacts and local protein structure (50, 51). A second possibility supported by our data is that the redistribution of R124H mutant TGFBI to lysosomes results in subcellular segregation of the proteins, decreasing their overall ability to interact in the cell.

Similar to TGFBI, mutant transthyretin is also a nonglycosylated, secreted protein that accumulates into extracellular deposits (43). The secretory system has a robust quality control system that functions to recognize and degrade terminally misfolded proteins through a process called ER-associated degradation. Previous studies have established that mutant transthyretin is recognized, degraded via this pathway, and displays reduced secretion (43). In contrast to transthyretin, our analyses indicate that disease-associated mutations in TGFBI have no effect on its secretion. These data indicate that mutant TGFBI eludes the secretory pathway protein quality control systems, resulting in the aberrant secretion of a mutant protein.

Based on the interaction between TGFBI and periostin and the clearly disruptive effects of the R124H mutation, we analyzed the distribution and expression pattern of periostin in the cornea of normal and GCD II patients. We observed anti-periostin staining in the corneal epithelial layer of normal corneal tissue. Within the corneal epithelium, periostin appeared to be mostly within the cell body and was excluded from the nucleus. In contrast, in GCD II, periostin accumulated in mutant TGFBI stromal

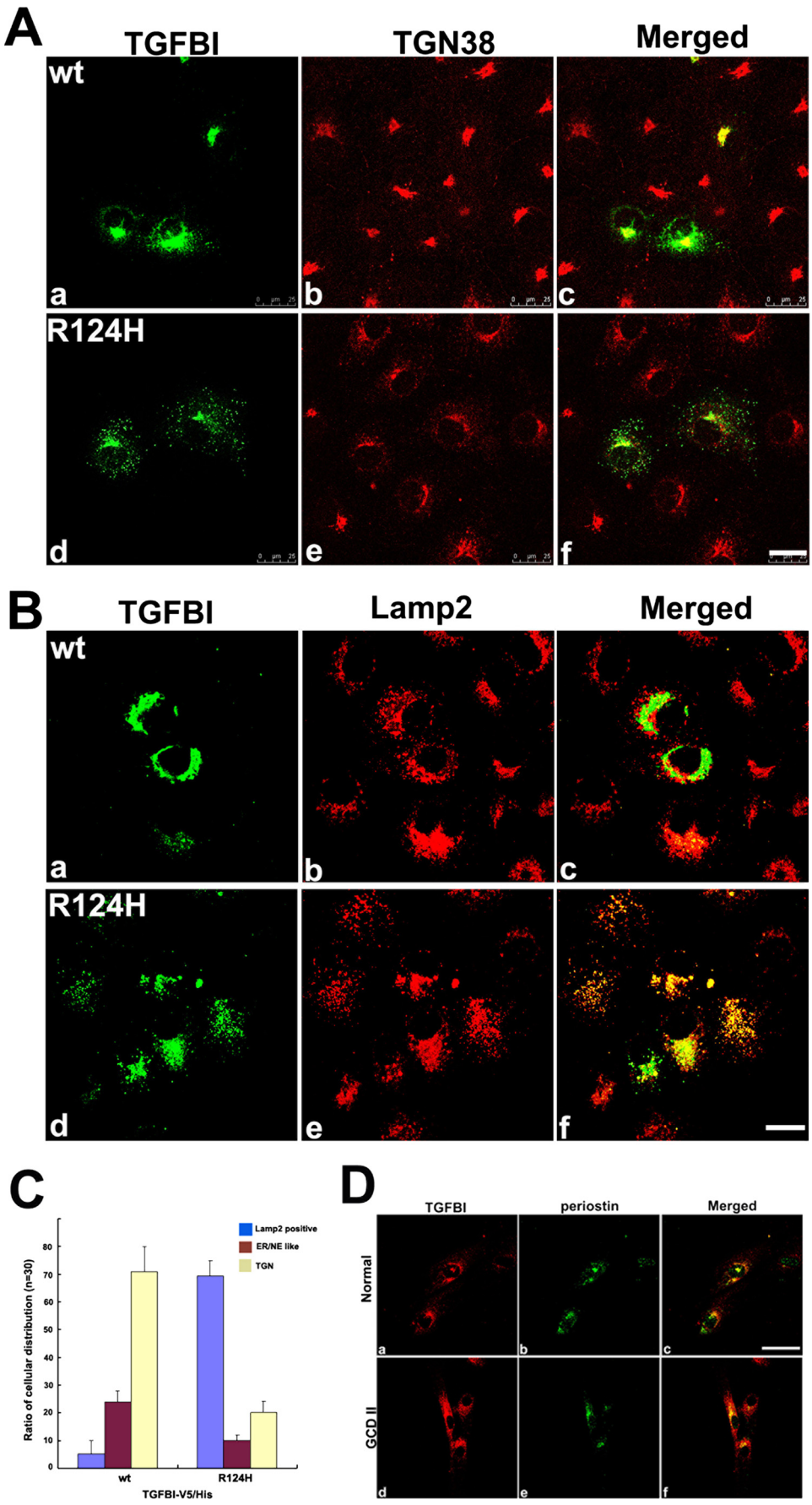

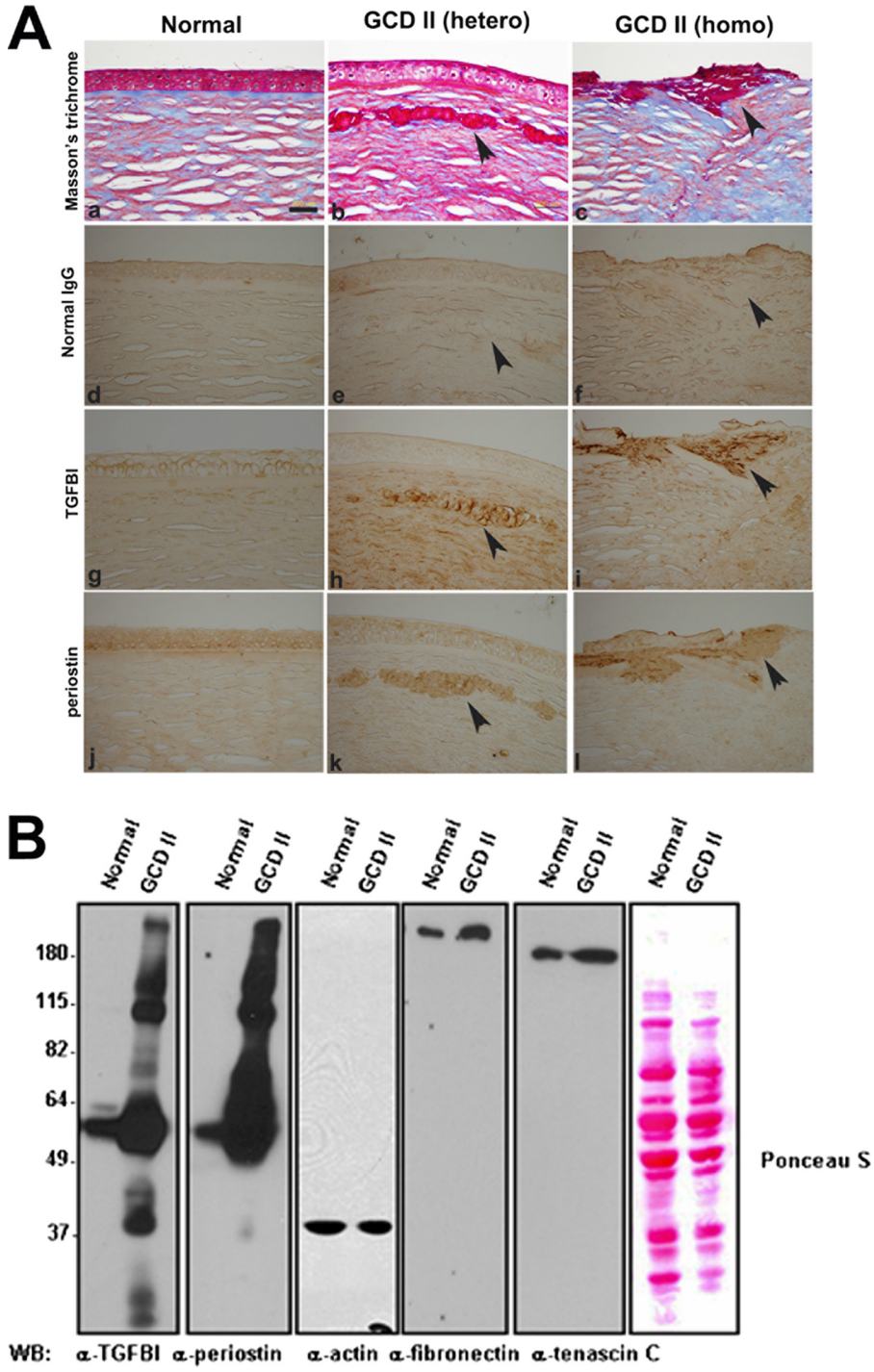

FIGURE 7. **Periostin accumulates in GCD type II-associated TGFBI corneal deposits.** *A*, corneas from a normal control (*a*, *d*, *g*, and *i*), a heterozygous GCD type II patient after lamellar keratoplasty (*b*, *e*, *h*, and *k*), and a homozygote GCD II patient (*c*, *f*, *i*, and *l*) were stained by Masson's trichrome (*a–c*), normal rabbit IgG (*d–f*), anti-TGFBI (*g–i*), and anti-periostin antibody (*j–l*). The *arrows* indicate the region of the TGFBI deposit. *Scale bar*, 200 μm. *B*, analysis of TGFBI and periostin expression in corneal epithelium extracts from normal human control and homozygous GCD II patients. Lysates were examined by Western blotting (*WB*) using the indicated antibodies.

deposits, which were highly granular in appearance and stained bright red with Masson's trichrome stain. Western blot analyses of corneal tissues from control and GCD II patients revealed a significant increase in the overall amounts of TGFBI and periostin in the diseased tissue. In addition, both TGFBI and periostin accumulated into a high molecular weight smear, suggesting that these proteins are in an aggregated form that is resistant to SDS denaturation. Not all ECM proteins showed this pattern. ECM proteins tenascin C, fibronectin, and collagens I and VI (Fig. 7) (data not shown) did not exhibit any changes in levels or molecular weight, indicating that not all TGFBI-interacting ECM proteins accumulate into the corneal deposits. Our results demonstrate that the TGFBI-interacting protein periostin is a specific component of the mutant TGFBI deposits in GCD II.

Our studies indicate that TGFBI and periostin are expressed in both corneal fibroblast and corneal epithelial cell types. Moreover, our corneal epithelial explants contain epithelial tissue and stromal tissue and show a mix of both the large and small form of periostin (Fig. 7), suggesting that periostin secreted from corneal fibroblasts and epithelial cells accumulates in the extracellular deposits observed in these patients. Together, these data support the validity and importance of our studies in these cell types. In the studies reported here, we have focused on TGFBI and periostin in corneal epithelial cells and COS-7 as a model cell line. Further studies with corneal epithelium would be of value for understanding the role of TGFBI and periostin. In summary, our findings reveal that periostin is a novel binding partner of TGFBI and

FIGURE 6. **GCD type II-associated R124H mutation in TGFBI causes mislocalization to the lysosome.** *A* and *B*, COS-7 cells expressing V5/His-tagged wild type or R124H mutant of TGFBI were immunostained with primary antibodies against V5 and TGN38 (*a–c*) or Lamp2 (*d–f*) and analyzed by confocal fluorescence microscopy. The *yellow color* indicates overlapping localization in the merged image. *C*, quantification of subcellular distribution of V5/His-tagged wild type and R124H mutant of TGFBI in COS-7 cells. COS-7 cells expressing V5/His-tagged wild type or R124H mutant TGFBI were immunostained with primary antibodies against V5 and TGN38 or Lamp2. Cellular distribution of TGFBI was determined based upon the colocalization of TGFBI with TGN38 or Lamp2. Data represent mean ± S.E. from three independent experiments. *D*, primary cultured corneal fibroblasts from a normal control (*a–c*) and a GCD II patient (*d–f*) bearing homozygous R124H mutations in TGFBI were fixed, permeabilized, and immmunostained with monoclonal anti-TGFBI (*red*) and polyclonal anti-periostin (*green*) antibodies. Cells were examined by confocal fluorescence microscopy. *Scale bars*, 50 μm.

that impairment of interaction of TGFBI with periostin by the corneal dystrophy-associated mutations in TGFBI may be involved in pathogenesis of 5q31-linked corneal dystrophies.

Acknowledgments—We thanks Drs. Hirokazu Inoue, Xiao-Fan Wang, In-San Kim, Shigeru Kinoshita, and James, V. Jester for essential reagents.

REFERENCES

1. Stone, E. M., Mathers, W. D., Rosenwasser, G. O., Holland, E. J., Folberg, R., Krachmer, J. H., Nichols, B. E., Gorevic, P. D., Taylor, C. M., and Streb, L. M. (1994) *Nat. Genet.* **6,** 47–51
2. Munier, F. L., Korvatska, E., Djemaï, A., Le Paslier, D., Zografos, L., Pescia, G., and Schorderet, D. F. (1997) *Nat. Genet.* **15,** 247–251
3. Kannabiran, C., and Klintworth, G. K. (2006) *Hum. Mutat.* **27,** 615–625
4. Korvatska, E., Munier, F. L., Djemaï, A., Wang, M. X., Frueh, B., Chiou, A. G., Uffer, S., Ballestrazzi, E., Braunstein, R. E., Forster, R. K., Culbertson, W. W., Boman, H., Zografos, L., and Schorderet, D. F. (1998) *Am. J. Hum. Genet.* **62,** 320–324
5. Pieramici, S. F., and Afshari, N. A. (2006) *Curr. Opin. Ophthalmol.* **17,** 361–366
6. Poulaki, V., and Colby, K. (2008) *Semin. Ophthalmol.* **23,** 9–17
7. Korvatska, E., Munier, F. L., Chaubert, P., Wang, M. X., Mashima, Y., Yamada, M., Uffer, S., Zografos, L., and Schorderet, D. F. (1999) *Invest. Ophthalmol. Vis. Sci.* **40,** 2213–2219
8. Mashima, Y., Nakamura, Y., Noda, K., Konishi, M., Yamada, M., Kudoh, J., and Shimizu, N. (1999) *Arch. Ophthalmol.* **117,** 90–93
9. Okada, M., Yamamoto, S., Tsujikawa, M., Watanabe, H., Inoue, Y., Maeda, N., Shimomura, Y., Nishida, K., Quantock, A. J., Kinoshita, S., and Tano, Y. (1998) *Am. J. Ophthalmol.* **126,** 535–542
10. Dighiero, P., Niel, F., Ellies, P., D'Hermies, F., Savoldelli, M., Renard, G., Delpech, M., and Valleix, S. (2001) *Ophthalmology* **108,** 818–823
11. Streeten, B. W., Qi, Y., Klintworth, G. K., Eagle, R. C., Jr., Strauss, J. A., and Bennett, K. (1999) *Arch. Ophthalmol.* **117,** 67–75
12. Takács, L., Boross, P., Tözser, J., Módis, L., Jr., Tóth, G., and Berta, A. (1998) *Exp. Eye Res.* **66,** 739–745
13. El-Ashry, M. F., Abd El-Aziz, M. M., Larkin, D. F., Clarke, B., Cree, I. A., Hardcastle, A. J., Bhattacharya, S. S., and Ebenezer, N. D. (2003) *Br. J. Ophthalmol.* **87,** 839–842
14. El Kochairi, I., Letovanec, I., Uffer, S., Munier, F. L., Chaubert, P., and Schorderet, D. F. (2006) *Mol. Vis.* **12,** 461–466
15. Skonier, J., Neubauer, M., Madisen, L., Bennett, K., Plowman, G. D., and Purchio, A. F. (1992) *DNA Cell Biol.* **11,** 511–522
16. Thapa, N., Lee, B. H., and Kim I. S. (2007) *Int. J. Biochem. Cell Biol.* **39,** 2183–2194
17. Doliana, R., Bot, S., Bonaldo, P., and Colombatti, A. (2000) *FEBS Lett.* **484,** 164–168
18. Runager, K., Enghild, J. J., and Klintworth, G. K. (2008) *Exp. Eye Res.* **87,** 298–299
19. Rawe, I. M., Zhan, Q., Burrows, R., Bennett, K., and Cintron, C. (1997) *Invest. Ophthalmol. Vis. Sci.* **38,** 893–900
20. Bastiani, M. J., Harrelson, A. L., Snow, P. M., and Goodman, C. S. (1987) *Cell* **48,** 745–755
21. Lindsley, A., Li, W., Wang, J., Maeda, N., Rogers, R., and Conway, S. J. (2005) *Gene Expr. Patterns* **5,** 593–600
22. Billings, P. C., Whitbeck, J. C., Adams, C. S., Abrams, W. R., Cohen, A. J., Engelsberg, B. N., Howard, P. S., and Rosenbloom, J. (2002) *J. Biol. Chem.* **277,** 28003–28009
23. Reinboth, B., Thomas, J., Hanssen, E., and Gibson, M. A. (2006) *J. Biol. Chem.* **281,** 7816–7824
24. Hanssen, E., Reinboth, B., and Gibson, M. A. (2003) *J. Biol. Chem.* **278,** 24334–24341
25. Kim, J. E., Park, R. W., Choi, J. Y., Bae, Y. C., Kim, K. S., Joo, C. K., and Kim, I. S. (2002) *Invest. Ophthalmol. Vis. Sci.* **43,** 656–661
26. Kim, J. E., Jeong, H. W., Nam, J. O., Lee, B. H., Choi, J. Y., Park, R. W., Park, J. Y., and Kim, I. S. (2002) *J. Biol. Chem.* **277,** 46159–46165
27. Nam, J. O., Kim, J. E., Jeong, H. W., Lee, S. J., Lee, B. H., Choi, J. Y., Park, R. W., Park, J. Y., and Kim, I. S. (2003) *J. Biol. Chem.* **278,** 25902–25909
28. Nam, E. J., Sa, K. H., You, D. W., Cho, J. H., Seo, J. S., Han, S. W., Park, J. Y., Kim, S. I., Kyung, H. S., Kim, I. S., and Kang, Y. M. (2006) *Arthritis Rheum.* **54,** 2734–2744
29. Kim, H. J., and Kim, I. S. (2008) *Int. J. Biochem. Cell Biol.* **40,** 991–1004
30. Park, S. J., Park, S., Ahn, H. C., Kim, I. S., and Lee, B. J (2004) *Peptides* **25,** 199–205
31. Takeshita, S., Kikuno, R., Tezuka, K., and Amann, E. (1993) *Biochem. J.* **294,** 271–278
32. Kudo, Y., Siriwardena B. S., Hatano, H., Ogawa, I., and Takata, T. (2007) *Histol. Histopathol.* **22,** 1167–1174
33. Horiuchi, K., Amizuka, N., Takeshita, S., Takamatsu, H., Katsuura, M., Ozawa, H., Toyama, Y., Bonewald L. F., and Kudo, A. (1999) *J. Bone Miner. Res.* **14,** 1239–1249
34. Yoshioka, N., Fuji, S., Shimakage, M., Kodama, K., Hakura, A., Yutsudo, M., Inoue, H., and Nojima, H. (2002) *Exp. Cell Res.* **279,** 91–99
35. Bao, S., Ouyang, G., Bai, X., Huang, Z., Ma, C., Liu, M., Shao, R., Anderson, R.M., Rich, J. N., and Wang X. F. (2004) *Cancer Cell.* **5,** 329–339
36. Kühn, B., del Monte, F., Hajjar, R. J., Chang, Y. S., Lebeche, D., Arab, S., and Keating, M. T. (2007) *Nat. Med.* **13,** 962–969
37. Butcher, J. T., Norris, R. A., Hoffman, S., Mjaatvedt, C. H., and Markwald, R. R. (2007) *Dev. Biol.* **302,** 256–266
38. Shimazaki, M., Nakamura, K., Kii, I., Kashima, T., Amizuka, N., Li, M., Saito, M., Fukuda, K., Nishiyama, T., Kitajima, S., Saga, Y., Fukayama, M., Sata, M., and Kudo, A. (2008) *J. Exp. Med.* **205,** 295–303
39. Takayama, G., Arima, K., Kanaji, T., Toda, S., Tanaka, H., Shoji, S., McKenzie, A. N., Nagai, H., Hotokebuchi, T., and Izuhara, K. (2006) *J. Allergy Clin. Immunol.* **118,** 98–104
40. Jester, J. V., Huang, J., Fisher, S., Spiekerman, J., Chang, J. H., Wright, W. E., and Shay, J. W. (2003) *Invest. Ophthalmol. Vis. Sci.* **44,** 1850–1858
41. Araki-Sasaki, K., Ohashi, Y., Sasabe, T., Hayashi K., Watanabe, H., Tano, Y., and Handa, H. (1995) *Invest. Ophthalmol. Vis. Sci.* **36,** 614–621
42. Gillan, L., Matei, D., Fishman, D. A., Gerbin, C. S., Karlan, B. Y., and Chang, D. D. (2002) *Cancer Res.* **62,** 5385–5394
43. Sekijima, Y., Wiseman, R. L., Matteson, J., Hammarström, P., Miller, S. R., Sawkar, A. R., Balch, W. E., and Kelly, J. W. (2005) *Cell* **121,** 73–85
44. Kern, C. B., Hoffman, S., Moreno, R., Damon, B. J., Norris, R. A., Krug, E. L., Markwald, R. R., and Mjaatvedt, C. H. (2005) *Anat. Rec. A Discov. Mol. Cell. Evol. Biol.* **284,** 415–423
45. Ma, C., Rong, Y., Radiloff, D. R., Datto, M. B., Centeno, B., Bao, S., Cheng, A. W., Lin, F., Jiang, S., Yeatman, T. J., and Wang, X. F. (2008) *Genes Dev.* **22,** 308–321
46. Callebaut, I., Mignotte, V., Souchet, M., and Mornon, J. P. (2003) *Biochem. Biophys. Res. Commun.* **300,** 619–623
47. Brodsky, J. L., and Scott, C. M. (2007) *Autophagy* **3,** 623–625
48. Lee, S. H., Bae, J. S., Park, S. H., Lee, B. H., Park, R. W., Choi, J. Y., Park, J. Y., Ha, S. W., Kim, Y. L., Kwon, T. H., and Kim, I. S. (2003) *Kidney Int.* **64,** 1012–1021
49. Kim, B. Y., Krämer, H., Yamamoto, A., Kominami, E., Kohsaka, S., and Akazawa, C. (2001) *J. Biol. Chem.* **276,** 29393–29402
50. Clout, N. J., Tisi, D., and Hohenester, E. (2003) *Structure* **11,** 197–203
51. Clout, N. J., and Hohenester, E. (2003) *Mol. Vis.* **9,** 440–448